# Magnetic Dichroism in the Angular Distribution of Atomic Oxygen 2$p$ Photoelectrons

O. Plotzke,[1] G. Prümper,[1] B. Zimmermann,[1] U. Becker,[1] and H. Kleinpoppen[2]

[1]*Fritz-Haber-Institut der Max-Planck-Gesellschaft, D-14195 Berlin, Germany*
[2]*Atomic Physics Laboratory, University of Stirling, Stirling FK9 4LA, Scotland*

A substantial difference in the angular distributions of 2$p$ photoelectrons from polarized oxygen atoms was found for two antiparallel atomic polarizations. This magnetic dichroism was studied as a function of photon energy from 25 to 52 eV. Our method extends traditional photoelectron angular distribution measurements of open shell atoms to "complete" experiments in similar to spin-resolved measurements. The observed dichroism allows a determination of the dipole matrix elements for the $\epsilon s$ and $\epsilon d$ photoelectrons and their phase difference including the sign. [S0031-9007(96)01267-7]

PACS numbers: 32.80.Fb

Photoionization and atomic collision processes can be completely described quantum mechanically by a limited number of amplitudes and their phase differences and thus the experiment from which the relevant amplitudes and phases can be extracted has been referred to as a *"complete"* experiment [1,2]. This possibility was first realized in the early electron-atom collision experiments of Eminyan *et al.* [3] and Standage and Kleinpoppen [4]. The first complete experiment in photoionization of atoms in the dipole approximation was reported by Heinzmann and co-workers [5,6], who measured the angular distribution and the spin polarization of photoelectrons for Xe 5$p$ photoionization. The complete information in the latter experiment is obtained from the spin polarization of the photoelectron (providing up to three further parameters of the photoionization process besides the cross section and angular distribution). The first experiment of this kind was followed by a series of further studies with a main emphasis on rare gas atoms. A complementary method for complete atomic photoionization experiments employs the polarization of the target atoms. The sensitivity of this method to additional photoionization parameters depends on the target preparation instead of the detection sensitivity to spin polarization. We refer for this class of experiments to the work of Klar and Kleinpoppen concerning the complete analysis of the relevant amplitudes and phases [7]. Successful experiments using polarized targets have first been reported [8–11] using laser excitation for the preparation of the initial state. However, these experiments focused predominantly on resonant photoionization processes where the information on matrix elements and phases is largely reduced. An alternative approach to such a complete analysis of nonresonant photoionization has been reported by Hausmann *et al.* [12] and Becker [13]; in their photoionization experiments on atomic magnesium and argon the angular distributions of the photoelectrons and Auger electrons provide the angular distribution asymmetry parameter $\beta$ and the alignment parameter $A_{20}$. These quantities together with the partial photoionization cross section $\sigma$ make it possible to derive matrix elements for continuum $s$ and $d$ electrons and

the cosine of their relative phase. Related experiments employ the polarization of the fluorescence radiation instead of the angular distribution of the Auger electrons [14]. A new type of complete photoionization experiments of this kind has only recently been reported based upon a coincidence analysis of photoelectrons and flourescence photons from the decay of exited $^2P_{3/2}$-state ions [15,16]. Using a combination of linearly and circularly polarized synchrotron radiation for the ionization provided relative $s$- and $d$-wave amplitudes and their phase differences (including the sign) [17].

The theoretical model in which the latter experiments may be regarded as complete is the validity of $LS$ coupling which is a good approximation in the case of photoionization of light atoms. The necessity of subsequent Auger or flourescence decay, however, limits these methods to inner-shell photoionization. Considering such studies for the valence shell, target polarization is, besides spin polarization measurement, the only possible method to obtain additional information on the photoionization process beyond $\sigma$ and $\beta$.

In this Letter we report on measurements of the angular distribution of photoelectrons from the reaction $O(2p^4) \times {}^3P_2 + h\nu \rightarrow O^+(2p^3)^4S_{3/2} + e^-$ by using $J$-polarized oxygen atoms and linearly polarized synchrotron radiation. The intensity difference between photoelectrons emitted from antiparallel polarized atoms is known as magnetic dichroism. Figure 1 shows the scheme of the apparatus applied. A 27 MHz discharge tube [18] has been used to dissociate the molecular oxygen into an atomic component of about 30% efficiency, yielding approximately $10^{17}$ atoms/s. After appropriate collimation, an atomic beam of oxygen atoms passes a hexapole magnet which focuses [19] the atoms with positive magnetic quantum numbers $M_J$ while those with negative $M_J$ are defocused. The hexapole magnet (pole-tip field strength 1.0 T, length 105 mm, diameter 14 mm) consists of 24 different parts to minimize fringe-field losses. The atoms leaving the strong field of the hexapole magnet approach adiabatically the weak field region. The vacuum chamber contains two concentric Mu-metal cylinders in
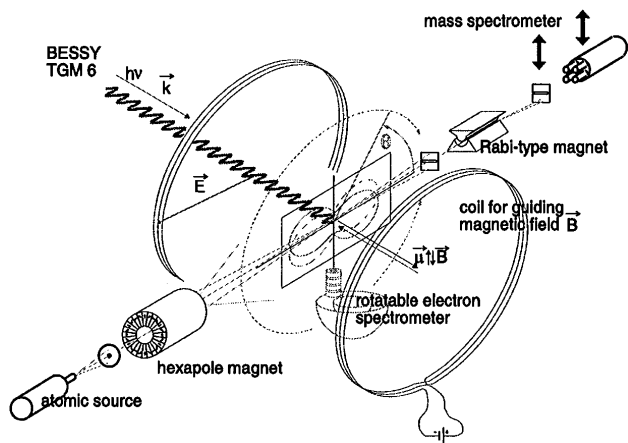
FIG. 1. Schematic of the experiment including the atomic source, a collimator, the hexapole magnet, the rotatable electron spectrometer, a Rabi magnet, mass spectrometer, the incoming synchrotron radiation from BESSY TGM6, and the magnetic coil pair for the guiding field.

order to shield the magnetic earth field of 44 $\mu$T. The remaining magnetic field of 1 $\mu$T is further compensated ($<0.1$ $\mu$T) by three orthogonal pairs of coils (not drawn in Fig. 1). In order to define the orientation of the atomic polarization and to have sufficient polarization of the atoms at the crossing point of the atomic beam with the ionizing synchrotron radiation, a guiding magnetic field of 2 $\mu$T is required, which is small enough to avoid a serious influence on the electron spectrometer. This influence was measured using unpolarized targets like He, Ne, or $O_2$. This field parallel to the synchrotron beam axis is provided by a further pair of magnetic coils. A rotatable electrostatic hemispherical electron spectrometer is used for the detection of the photoelectrons; its mean radius is 50 mm and its mean energy resolution at 10 eV pass energy was measured to 150 meV. This value is optimized for the energy sharpness of about 150 meV of the synchrotron radiation applied for the nonresonant measurements (undulator beam line U1-TGM6 at BESSY). The undulator gap was adjusted to give maximum flux ($10^{14}$–$10^{12}$ photon/s) at each particular photon energy and a high degree of linear polarization (typical undulator gaps 35 to 50 mm). The degree of linear polarization was determined to $P_1 = 0.99 \pm 0.01$ by analyzing the He $1s$ photoelectron angular distribution. Following a construction of the polarized atomic beam apparatus of Stirling University [19], a new Rabi magnet has been developed to monitor the polarization of the atomic beam by studying the components of the Stern-Gerlach splitting. The relative intensities $g_{M_J}$ of these components have been analyzed for atomic oxygen by a numerical Monte Carlo simulation of the thermal beam which reproduces the Stern-Gerlach profiles: $M_J = -2, -1, 0, 1, 2$, 3%, 7%, 13%, 24%, 53%, respectively. Photoionization of the $s$ and $p$ shells has been studied at five angular positions of the electron spectrometer, namely, 0°, 40°, 225°, 270°, and 315°:

$$O(1s^2 2s^2 2p^4)^3P_2 + h\nu \rightarrow O^+(1s^2 2s^1 2p^4)^4P_2 + e^-, \tag{1}$$

$$O(1s^2 2s^2 2p^4)^3P_2 + h\nu \rightarrow O^+(1s^2 2s^2 2p^3)^4S_{3/2} + e^-. \tag{2}$$

The guiding magnetic fields $\vec{B}$ for the polarization direction of the atoms were parallel $\vec{B} \uparrow\uparrow \vec{k}$ or antiparallel $\vec{B} \downarrow\uparrow \vec{k}$ to the propagation vector $\vec{k}$ of the incoming light. To avoid long term effects, the two photoelectron spectra where taken almost simultaneously, by inverting the magnetic field every second. The angular distribution of the photoelectron count rate in the detector plane of Fig. 1 can be parametrized as follows (for a linear polarization $P_1 \leq 1$ of the synchrotron radiation):

$$I_\pm(\Theta) = C_I \frac{d\sigma_\pm}{d\Omega}(\Theta)$$

$$= C_I \frac{\sigma}{4\pi} \left[ c_1 \left( 1 + \frac{\beta}{4}[1 + 3P_1 \cos(2\Theta)] \right) \right.$$

$$\left. \pm c_2 \beta' P_1 \sin(2\Theta) \right]$$

with $c_1 = \frac{3}{2} g_2 + \frac{3}{4} g_1 + \frac{1}{2} g_0 + \frac{3}{4} g_{-1} + \frac{3}{2} g_{-2}$

$$\approx 1.14$$

and $c_2 = g_2 + \frac{1}{2} g_1 - \frac{1}{2} g_{-1} - g_{-2} \approx 0.585$. (3)

All nondipole contributions are neglected, because they either vanish in the detector plane or are smaller by several orders of magnitude [20]. The factor $C_I$ includes the target density, reaction volume, detection efficency, light intensity, etc. The factors $c_1$ and $c_2$ depend on the $M_J$-population numbers mentioned above. The positive sign of the last term refers to the case $\vec{B} \uparrow\uparrow \vec{k}$, the negative one to $\vec{B} \downarrow\uparrow \vec{k}$. This enables us to measure $\beta$ and $\beta'$ in the photon energy range from about 25 to 52 eV. The sum of both count rates $I_+(\Theta)$ and $I_-(\Theta)$ gives the common $\beta$ distribution for unpolarized targets. The product $C_I \sigma$ can be fitted by the angular distribution of the sum of these for given $\beta$. $\beta$ is determined from measurements with unpolarized atoms and was found to be compatible with our distribution. The count rate difference is

$$I_+(\Theta) - I_-(\Theta) = C_I \frac{\sigma}{4\pi} c_2 \beta' P_1 \sin(2\Theta), \tag{4}$$

which determines the $\beta'$ parameter with the knowledge of $C_I \sigma$ and $P_1$. Alternatively $\beta'$ can be calculated from the dichroism measured at the quasimagical angle $\Theta_{\text{mag}}$ without using $C_I \sigma$ or $\beta$:

$$\frac{I_+(\Theta_{\text{mag}}) - I_-(\Theta_{\text{mag}})}{I_+(\Theta_{\text{mag}}) + I_-(\Theta_{\text{mag}})} = \frac{c_2}{2c_1} P_1 \beta' \sin(2\Theta_{\text{mag}})$$

$$\text{with } \Theta_{\text{mag}} = \frac{1}{2} \cos^{-1}\left(-\frac{1}{3P_1}\right). \tag{5}$$
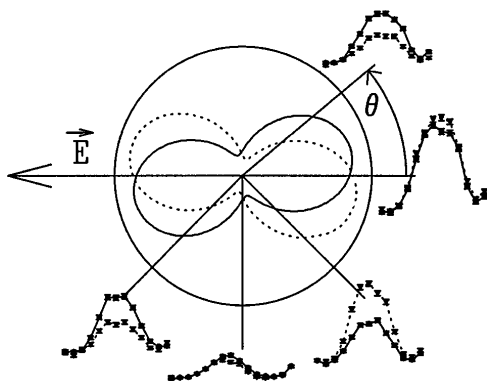
Figure 2 shows an example of the distinct "linear mag-

FIG. 2.  Magnetic dichroism in the angular distribution for the $2p$ photoionization of atomic oxygen for different photoelectron detection angles $\Theta$ and a photon energy $h\nu = 30.5$ eV. The spectra depicted by solid lines are for $\vec{B} \uparrow\uparrow \vec{k}$ (magnetic guiding field parallel to the propagation vector of the synchrotron radiation) while the dashed lines show the antiparallel case $\vec{B} \downarrow\uparrow \vec{k}$.



FIG. 3.  Angular distribution parameters $\beta$ and $\beta'$, the difference in asymptotic phase shift and the partial wave amplitudes. The dotted curves are the theoretical result using the Cowan code [21], the dash-dotted curves represent theoretical results from Ref. [29], and the $\beta$ values below 25 eV are from Ref. [27]. The solid line represents the quantum defect difference of the two $ns$ and $nd$ Rydberg series which converge to the $^4S$ threshold.

netic dichroism" in the angular distribution of the photoionization of a $2p$ electron of atomic oxygen [reaction (2)]. Contrary to this in the angular photoelectron distribution of reaction (1) no such dichroism was experimentally observed, which is expected since only relativistic effects cause dichroism for $s$ electrons. The same is true for atomic hydrogen, which was produced in the same source. With the nozzle cooled to 100 K the hydrogen atoms follow the same trajectories as oxygen atoms with room temperature velocity distribution.

In order to interpret the data for the photoelectrons of the reaction $O(2p^4)^3P_2 + h\nu \rightarrow O^+(2p^3)^4S_{3/2} + e^-$ we describe the angular distribution of this open shell atom in $LS$ coupling. Neglecting relativistic effects the measurements of the parameters $\beta$ and $\beta'$ can be used to determine the ratio $\gamma = R_d/R_s$ of the two radial components of the matrix elements for the $2p$ electron photoionized into $\epsilon s$ and $\epsilon d$ continuum states and the difference in asymptotic phase shifts $\Delta = \Delta_d - \Delta_s$ of these states. The following equations for transformation between $(\beta, \beta')$ and $(\gamma, \Delta)$ can be used:

$$\beta_{O\,2p^4 S_{3/2}} = \frac{\gamma[2\gamma + 4\cos(\Delta)]}{1 + 2\gamma^2} \qquad (6)$$

$$\beta'_{O\,2p^4 S_{3/2}} = -\frac{3\gamma \sin(\Delta)}{1 + 2\gamma^2}. \qquad (7)$$

Similar equations hold for the final ionic states $^2D$ and $^2P$. Possible contributions from the excited fine-structure states $^3P_1$ and $^3P_0$ (gas temperature 300 K) were not resolved. They affect the factors $c_1$ and $c_2$ only weakly, so the determination of $\gamma$ and $\Delta$ is possible without knowing the exact population numbers of the fine-structure multiplet.

The results of the transformation $(\beta, \beta') \rightarrow (\gamma, \Delta)$ are shown in Fig. 3, along with theoretical calculations using the Cowan code [21]. The transformation to absolute amplitudes by
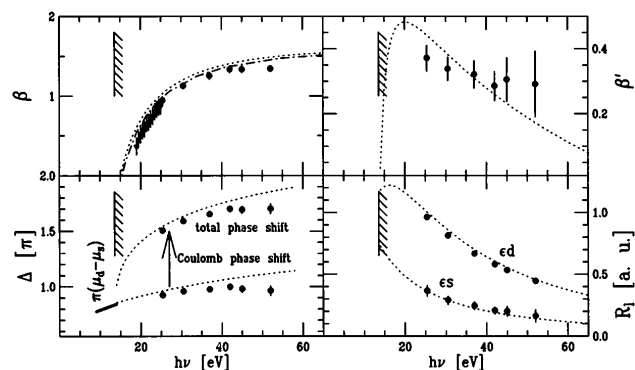
$$\sigma = \frac{4\pi^2\alpha}{3} h\nu \frac{R_s^2 + 2R_d^2}{3} \qquad (8)$$

($\sigma$ in units of $a_0^2$, $h\nu$ in Ry, and $R_s$ and $R_d$ in a.u.) was made using an exponential fit through the absolute $2p\,^4S$ cross section data from [22] involving a systematic error of 10%. As $\beta$ and $\beta'$ are independent quantities, it is not possible to calculate one from the other. However, the result of the transformation $(\beta, \beta') \rightarrow (\gamma, \Delta)$ is not unique, as generally the curves of constant $\beta$ and $\beta'$ meet in two points. Even though the number of independent measurements equals the number of free parameters one bit of information is still missing. Far from threshold the $d$ amplitude is expected to exceed the $s$ amplitude, and therefore one of the solutions can be ignored. In this case ($\Delta \approx 270°$) the large error bar of $\beta'$ only affects the error bar of $\gamma$. While the ratio of the radial dipole integrals is almost constant for $h\nu$ from 25 to 52 eV, the total difference in the asymptotic phase shifts $\Delta$ changes more than 30° in this regime. This is mainly due to the difference in Coulomb phase shifts for the two different angular momenta. If the Coulomb phase shift between the $d$ and $s$ wave is subtracted from $\Delta$, the intrinsic phase shift agrees well with the extrapolation of the quantum defect function below the ionization threshold. The corresponding values have been calculated from Ref. [23]. Former theoretical studies did not report the phase difference for the $^4S$ state; however, their $\beta$ results are in overall good agreement with our experimental and theoretical data [24].

The variations of $\sigma$, $\beta$, and $\beta'$ were measured also at the $2s2p^4 3p$ resonance. Assuming that only the $2s2p^4 3p\,^3D$ resonance contributes significantly, the individual count rates at different angles for different atomic polarizations were fitted using a Shore parametrization [25] of the Fano profile [26]. The monochromator energy width was about 30 meV, the Fano $q$ value for the absolute $2p\,^4S$ cross section is $-1.9 \pm 0.1$ which is consistent with [27]. The resulting profiles where used to calculate the $\beta$ and $\beta'$
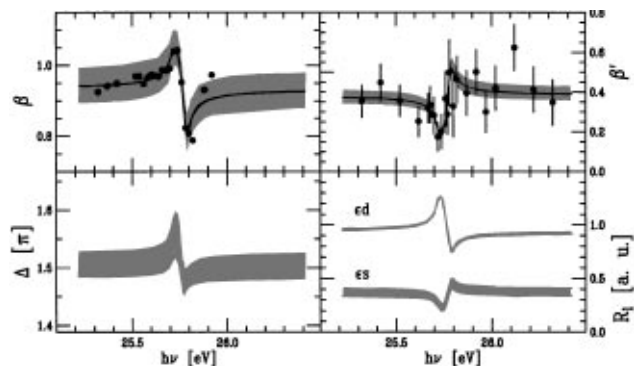
FIG. 4. Photoionization parameters and partial wave behavior within the autoionizing $2s2p^43p\,^3D$ resonance. The solid lines represent fit curves using a Shore parametrization of the resonance profiles. The error limits of this parametrization are represented by the shadowed zone.

curves. A weak resonance in the $\beta$ parameter and a strong resonance in the magnetic dichroism are observed and analyzed in terms of varying matrix elements and phases. Figure 4 shows the corresponding results. The analysis reveals an interesting feature of the resonance behavior of the two partial waves; their channel dependent "$q$" values [24,28] have different signs $q_d = -1.95 \pm 0.1$, $q_s = 0.9 \pm 0.4$. This indicates a sign difference between the Coulomb matrix elements of the two $s$ and $d$ continua with the excited discrete state [30]. This is the first direct probe of the sign of a Coulomb or Auger matrix element describing the emission of a $l$-resolved nondegenerate continuum electron via Coulomb interaction.

Our measurements clearly demonstrate that traditional angle resolved photoelectron spectroscopy of open shell atoms can be extended to complete photoionization experiments by the use of polarized atomic beams. Our results show that besides greater complexity of open shell atoms their photoionization may be consistently described in terms of three parameters only depending on $LS$ coupling at least for lighter atoms. Regarding photoexcitation the method makes it possible to derive single channel dipole and Coulomb matrix elements within an autoionizing resonance.

[1] U. Fano, Rev. Mod. Phys. **29**, 74 (1957).

[2] B. Bederson, Comments At. Mol. Phys. **1**, 41 (1969); **2**, 65 (1969).

[3] M. Eminyan, K. MacAdam, J. Slevin, and H. Kleinpoppen, Phys. Rev. Lett. **31**, 576 (1973).

[4] M. C. Standage and H. Kleinpoppen, Phys. Rev. Lett. **36**, 577 (1976).

[5] U. Heinzmann, J. Phys. B **13**, 4367 (1980).

[6] C. Heckenkamp, F. Schäfers, G. Schönhense, and U. Heinzmann, Phys. Rev. Lett. **52**, 421 (1984).

[7] H. Klar and H. Kleinpoppen, J. Phys. B **15**, 933 (1982).

[8] A. Siegel, J. Ganz, W. Bussert, and H. Hotop, J. Phys. B **16**, 2945 (1983).

[9] C. Kerling, N. Böwering, and U. Heinzmann, J. Phys. B **23**, L629 (1990).

[10] M. Pahler, C. Lorenz, E. v. Raven, P. Rüder, B. Sonntag, S. Baier, B. R. Müller, M. Schulze, H. Staiger, and P. Zimmermann, Phys. Rev. Lett. **68**, 2285 (1992).

[11] M. Wedowski, K. Godehusen, T. Dohrmann, F. Weisbarth, A. von dem Borne, P. Zimmermann, B. Sonntag, and A. N. Grum-Grzhimailo, J. Electron Spectrosc. Relat. Phenom. **75**, 61 (1995).

[12] A. Hausmann, B. Kämmerling, H. Kossmann, and V. Schmidt, Phys. Rev. Lett. **61**, 2669 (1988).

[13] U. Becker, in *The Physics of Electronic and Atomic Collisions,* edited by A. Dalgarno, R. S. Freund, P. M. Koch, M. S. Lubell, and T. B. Lucatorto (AIP, New York, 1990), p. 162.

[14] W. Kronast, R. Huster, and W. Mehlhorn, Z. Phys. D **2**, 285 (1986).

[15] H. Hamdy, H. J. Beyer, J. B. West, and H. Kleinpoppen, J. Phys. B **24**, 4957 (1991); H. J. Beyer, J. B. West, K. J. Ross, K. Ueda, N. W. Kabachnik, H. Hamdy, and H. Kleinpoppen, J. Phys. B **28**, L47 (1995).

[16] J. B. West, K. Ueda, N. W. Kabachnik, K. J. Ross, H. J. Beyer, and H. Kleinpoppen, Phys. Rev. A **53**, R9 (1996).

[17] N. W. Kabachnik and K. J. Ueda, J. Phys. B **28**, 5013 (1995).

[18] J. Slevin and W. Stirling, Rev. Sci. Instrum. **52**, 1780 (1981).

[19] M. A. H. Bukhari, H. J. Beyer, M. A. Chaudhry, D. M. Campbell, A. J. Duncan, H. Kleinpoppen, J. Phys. B **28**, 1889 (1995).

[20] J. W. Cooper, J. Phys. B **47**, 1841 (1993).

[21] R. D. Cowan, *The Theory of Atomic Structure and Spectra* (University of California Press, Berkeley, Los Angeles, London, 1981). We performed the calculation using the codes RCN and RCG.

[22] S. L. Schaphorst, M. O. Krause, C. D. Caldwell, H. P. Saha, M. Pahler, and J. Jimenez-Mier, Phys. Rev. A **52**, 4657 (1995).

[23] C. E. Moore, *Atomic Energy Levels,* National Bureau of Standards Circular Vol. 467 (National Bureau of Standards, Gaithersburg, MD, 1949), Vol. 1.

[24] A. F. Starace, Phys. Rev. A **16**, 231 (1977).

[25] B. W. Shore, Phys. Rev. **171**, 43 (1968).

[26] U. Fano, Phys. Rev. **124**, 1866 (1961); U. Fano and J. W. Cooper, *ibid.* **137**, 1364 (1965).

[27] P. van der Meulen, M. O. Krause, C. A. de Lange, Phys. Rev. A **43**, 5997 (1991).

[28] C. F. Farnoux, Phys. Rev. A **25**, 287 (1982).

[29] A. F. Starace, S. T. Manson, and D. J. Kennedy, Phys. Rev. A **9**, 2453 (1974).

[30] The channel dependent $q$ values are connected with the dipole and Coulomb matrix elements by

$$\frac{(1 + q_d q_s) + i(q_d - q_s)}{1 + q_d^2} = \frac{\alpha_s}{\alpha_d}$$

$$= \frac{\langle\phi|V|\mu_s\rangle}{\langle\phi|V|\mu_d\rangle}\frac{\langle g|\vec{r}|\mu_d\rangle}{\langle g|\vec{r}|\mu_s\rangle},$$

where $\mu_l$ are the continuum states that fulfill the incoming-wave boundary condition [24].